

Article

Lineaments in the Gravity Image of the Border Zone between the Central and Outer Carpathians

Sławomir Porzucek ^{*}, Monika Loj  and Jan Golonka

Faculty of Geology, Geophysics and Environmental Protection, AGH University of Kraków, 30 Mickiewicz Avenue, 30-059 Kraków, Poland; mloj@agh.edu.pl (M.L.); jgonlonka@agh.edu.pl (J.G.)

* Correspondence: porzucek@agh.edu.pl

Abstract: The research area covers the border zone between the Central and Outer Carpathians. The purpose of this research was the interpretation of this zone based on a gravitational survey. This survey was integrated with the results of surface mapping, a deep seismic survey, and deep drillings. Three major tectonic units are located in this area: the Outer (Flysch) Carpathians, the Pieniny Klippen Belt (PKB), and the Central Carpathians. All three units contain a significant amount of flysch sequences. The lowering of the Bouguer anomaly value from north to south reflects the dip of the crystalline European Plate; in turn, the renewed increase in value correlates very well with the emergence of the crystalline ALCAPA Plate. The range of variability of the Bouguer anomaly value largely masks smaller anomalies in amplitude originating from smaller geological structures. Only three anomalies with significant horizontal extent and greater amplitudes are visible: two are clearly correlated with the Orava-Nowy Targ Basin and the third anomaly is likely connected with the thicker pile of the Outer Carpathian flysch. To separate the boundaries of geological or tectonic structures (lineaments), a horizontal derivative (THDR) and an analytical signal (ASA) were used. Both methods allowed us to confirm existing geological and tectonic boundaries (lineaments) and to identify new ones.

Keywords: gravity; gravity anomaly; gravity derivatives; analytic signal; lineaments; Western Carpathian; Outer (Flysch) Carpathians; Pieniny Klippen Belt



Citation: Porzucek, S.; Loj, M.; Golonka, J. Lineaments in the Gravity Image of the Border Zone between the Central and Outer Carpathians. *Minerals* **2023**, *13*, 995. <https://doi.org/10.3390/min13080995>

Academic Editor: Michael S. Zhdanov

Received: 12 May 2023
Revised: 18 July 2023
Accepted: 25 July 2023
Published: 26 July 2023



Copyright: © 2023 by the authors. Licensee MDPI, Basel, Switzerland. This article is an open access article distributed under the terms and conditions of the Creative Commons Attribution (CC BY) license (<https://creativecommons.org/licenses/by/4.0/>).

1. Introduction

The research area is located in the Carpathian Mountains in southern Poland, south of Kraków, between Mszana Dolna and the foothills of the Tatra Mountains. The previous geological and geophysical studies of this area revealed the existence of two major structural units, the Central and Outer Carpathians, separated by the Pieniny Klippen Belt [1,2]. Several secondary tectonic units are separated by thrust faults, and transverse strike-slip faults were also distinguished in this area [3,4].

Geophysical research has been carried out in the Western Carpathians for many years. Among them, the most common are seismic surveys [5], particularly for the exploration of oil and gas deposits. For a deeper geological exploration, magnetotelluric studies were also carried out [6]. This area was also analyzed on the basis of gravity and magnetic studies [7]. The latter publication focuses on the general description of the recorded anomalies and an attempt to determine the morphology of the crystalline basement. In 2003, Pomianowski [8] presented gravimetric and geoelectric models along the profiles crossing the Orava-Nowy Targ Basin. Recently, more detailed analyses of gravity and magnetic studies of [9,10] for the westernmost Polish Outer Carpathians have also appeared. They used several gravity data processing procedures based on the filtering of the frequency domain.

In our publication a wide range of gravity data processing procedures were used that focused primarily on the search for lineaments. Basic gravity interpretation is conducted based on the distribution of Bouguer's anomaly [11]. Usually, in the next stage

of interpretation, the regional factor from larger, extensive structures is removed from Bouguer's anomaly [12]). This factor, calculated using upward continuation, allows one to obtain residual anomalies. These anomalies have a smaller amplitude and horizontal range and allows one to detect or better contour smaller, local structures and the separation of lineaments [13]. A necessary but not sufficient condition for detecting structures or lineaments is the existence of bulk density contrasts between the geological structure and its surroundings.

There are some processing methods which use gravity derivatives to determine geological structures and lineaments. The first gravity derivatives, in particular the gravity vertical derivative (VDR), emphasize the effects of shallow-lying structures and density boundaries. Gravity derivatives allowed us to calculate the total horizontal derivatives (THD) and analytic signals (ASA), which are widely used for lineament and structure boundary detection [14].

The goal of this research was the interpretation of the border zone between the Central and Outer Carpathians based on a gravitational survey [15]. This survey was integrated with the results of surface mapping, a deep seismic survey, and deep drillings. The geological field work allowed us to distinguish the main structural units in the investigated area [1]. Several deep drillings penetrated these units. The deep seismic survey [2] divulged the relationship between the major plates existing of this area. The character of the tectonic boundaries between geological units and the internal structures of these units is still controversial. We hope that studies of gravity anomalies could help unravel the details of tectonics, especially the position of major faults and other lineaments.

The type of morphology and geology in the research area represent classic *mélange*. The study of this *mélange* may fundamentally change our understanding of the regional geology, paleogeography, and paleodynamic evolution of this area, as well as those of other mountain belts. The research results may be useful in the hydrocarbon exploration in the Carpathians. The research area can be also treated as a geological field laboratory, with visible objects and processes helping to understand the earth's complex geological history. Better recognition of the geology of this region will increase its attractiveness as a training area for students and young scientists and as geotouristic object with outstanding cognitive qualities.

2. Outline of the Geological Setting

The research area belongs to the Carpathians that form a great mountain arc in Central Europe (Figure 1). The Western Carpathian structure was the result of a collision between the consolidated North European Plate and microplates included in the larger tectonic element ALCAPA (Alpine-Carpathian-Pannonian) [16–18].

ALCAPA includes the Alps, Carpathians, the Pannonian Basin, and other smaller basins (Figure 1). The microplates involved in the collision include the Central Western Carpathians and Inner Western Carpathians.

Three major tectonic units are located in this area: the Outer (Flysch) Carpathians, the Pieniny Klippen Belt (PKB), and the Central Carpathians. The PKB is located in the suture zone between the Central and Outer Carpathians. The Central Carpathians consists of Paleozoic granite and metamorphic rocks, as well as Mesozoic sedimentary rocks. These sedimentary rocks include mainly Triassic-Cretaceous carbonates.

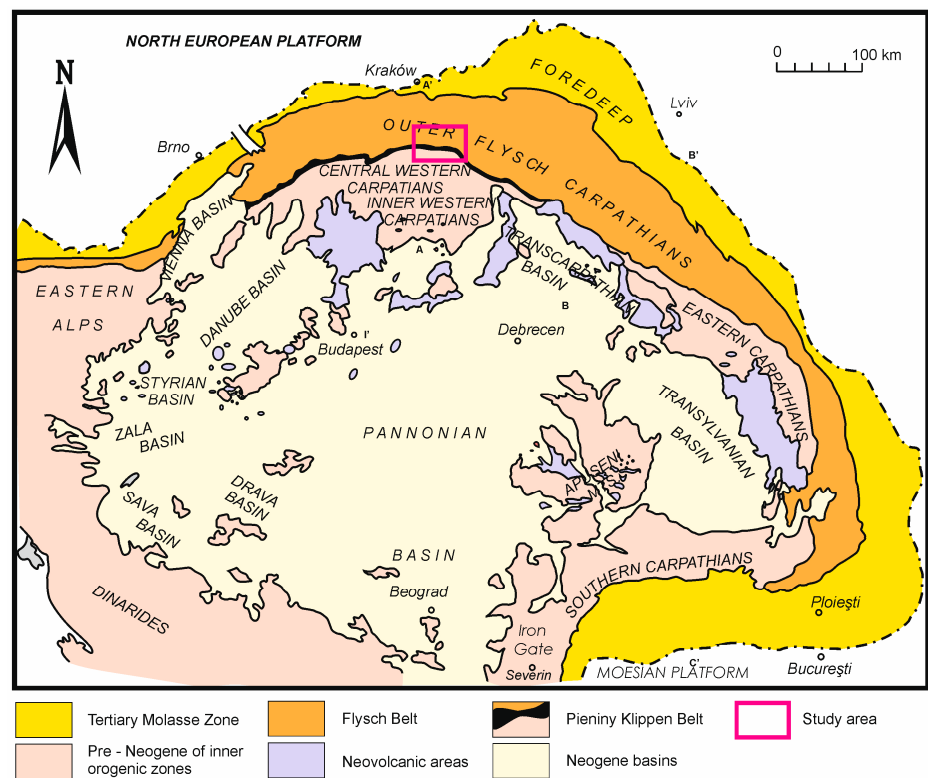


Figure 1. Location of the study area on a simplified geological map of the Carpathian chain within Europe. Modified after [19].

The Mesozoic-Cenozoic development of the Central Carpathians includes the deposition of an epicontinental platform and deeper pelagic sediments on the granitic and metamorphic basement. Late Cretaceous shortening caused nappe thrusting from the south to the north [3]. The Central Carpathian Paleozoic and Mesozoic rocks are exposed in the Tatra Mountains south of the research area. The Central Carpathian Paleogene covers these rocks north of the Tatras. It is represented by the Middle Eocene conglomerates and limestones, followed by 3000-m-thick Eocene-Oligocene flysch sequences (Podhale Flysch Basin). These sequences form a syncline between the Tatra Mountains and the border with the PKB [1]. The PKB is limited by deeply rooted faults on both sides that form the flower structure [20,21]. The Jurassic-Albian sedimentary sequences of the PKB are mainly represented by limestones and radiolarites. The flysch rocks were deposited during Albian-Neogene times. They contain olistoliths arranged in two belts. The mélangé character of PKB is expressed by complex tectonics that shows both nappes and deep-rooted faults, and by the occurrence of olistostrome and wildflysch [22].

The PKB and the Outer Carpathians are separated by a subvertical strike-slip fault. This suture zone is partially covered by the Neogene deposits of the Orava-Nowy Targ Basin. The thickness of sand-silt and clay, which were deposited in this Basin reaches 900 m. Some thin layers of coal intercalate faintly cemented silty clays. The age of the oldest sediments was established in the Carpathian-Badenian (Serravalian) [23]. The Orava-Nowy Targ Basin originated during strike-slip movements in the basement and is considered as a pull-apart basin [8,23]. The Miocene-Pliocene marine and fresh-water deposits are covered by Quaternary siliciclastics, mainly gravels.

The Outer Carpathians consist of the Upper Jurassic to the Lower Miocene flysch sequences, which are up to six kilometers thick. These sequences include turbiditic sandstones, mudstones, calcareous shales, and marlstones, sometimes with cherts and limestones. Olistoliths from various basement and ridge units and redeposited flysch packages are common [3,24]. The flysch sequences are thrust over the North European Plate, forming the fold-and-thrust belt.

The Outer Carpathian flysch is divided into several nappes and thrust sheets: the Magura Nappe, Fore-Magura group of nappes, and the Dukla, Silesian, Subsilesian, and Skole nappes (Figure 2). The southern large Magura Nappe is divided into four lithostratigraphic-tectonic units: Krynica, Bystrica, Rača, and Siary. All these units are built mainly of Lower Cretaceous to Oligocene flysch rocks. The southernmost Krynica Unit borders the PKB. The northern Outer Carpathian nappes built of Upper Jurassic to Lower Miocene flysch sequences are covered by the Magura Nappe in the research area. They are exposed only in the Mszana tectonic window. The North European Platform consists of the Precambrian crystalline basement and the Paleozoic-Miocene sedimentary cover [1,24]. The rocks of the Magura nappe are cut by several deep faults perpendicular to the strike of the nappe [25]. The Miocene andesitic dykes and sills are located near the PKB-Magura Nappe border (Figure 2). Intrusions cut through the Magura Nappe and the PKB form andesitic dykes and sills distributed along the Pieniny Andesitic Line (PAL) [22,26,27]. The sediments that form the Outer Carpathian nappes were originally deposited in the Mesozoic and Cenozoic basins belonging to the western part of the Tethyan realm [23,24]. The evolutionary stages of these basins include:

- Jurassic–Cenomanian syn-rift and post-rift, extension—opening of basins;
- Cenomanian–Eocene synorogenic, contraction, and collisional—development of subduction zones, partial closure of basin, destruction of ridges, sedimentation of synorogenic turbidites (flysch) formation, and development of accretionary prism;
- Eocene–Miocene late orogenic, contractional, collisional (Eocene–Miocene)—further development of accretionary prism closing of basins, final destruction of ridges, development of piggy-back basins.

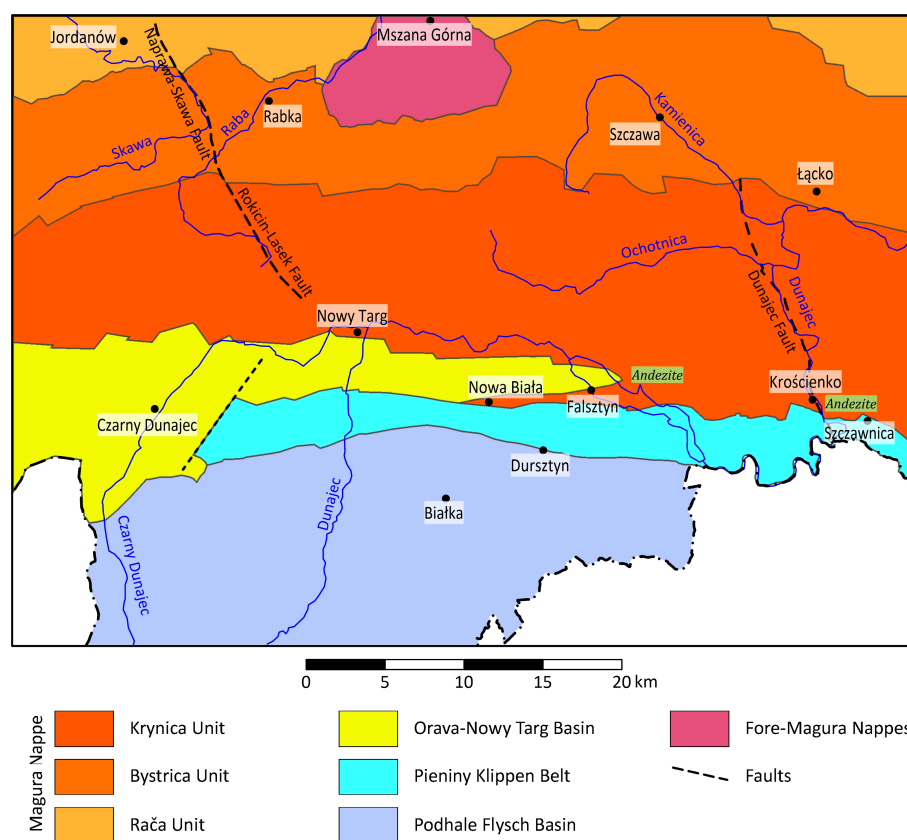


Figure 2. Simplified geology of the study area (created based on tectonic sketches from explanatory notes to the detailed geological map of Poland, sheets no.: 1032, 1033, 1034, 1048, 1049, 1050, 1060, 1061).

The main tectonic phase took place in the Miocene during the collision between the overriding ALCAPA plate and the North European plate. As a result of intense Neogene

orogeny, the sedimentary infill of the Outer Carpathian basins became folded and detached from its substratum. Several uprooted nappes and thrust-sheets were created. The Carpathian Foredeep was formed in front of the steeply northward-advancing nappes [23,24].

3. Methods

The gravity method, based on the natural gravitational field of the Earth, is used to identify change in the gravity field that reflect the changes in the density distribution in the rock mass, both in prospecting and engineering studies. In this paper, it is used, in particular, to identify edge structures, contacts, and lineaments. The Bouguer anomalies are a source of information on the distribution of this density and are calculated as the difference between the sum of the measured gravity value g with the Bouguer reduction to a reference level and the normal value of gravity g_N calculated at that level (latitude correction), using Formula (1).

$$\Delta g = g + \delta g_F + \delta g_B + \delta g_T - g_N \quad (1)$$

The Bouguer reduction consists of three corrections: terrain correction δg_T , free-air correction δg_F , and Bouguer correction δg_B [11,28] and is applied in order to eliminate from the observed gravity values the influence of changes in the topography of the terrain surface. After their introduction, it is possible to calculate the Bouguer anomaly (1) by subtracting the normal value of the gravity force g_N , which is calculated on the basis of the International Gravity Formula for the Earth model of the Geodetic Reference System 1980 [29].

The Bouguer anomaly is the sum of all gravity effects connected with all underground sources. How big those effects are depends on the source size and mass, and their distance from the observation points. For this reason, the interpretation of the Bouguer anomaly can be divided into two parts. Both of these parts are connected with separation problem techniques. As such, these techniques can be classified as isolation and enhancement methods of interpretation [30]. First, isolation techniques are used to isolate some parts of the anomaly from others. Generally, it means that the anomaly is divided into regional (large-scale) and residual (local-scale) anomalies, connected with deep sources (first) and shallow sources (second). On the other hand, using the enhancement techniques makes it possible to bring out significant anomalies and accent their perceptibility. The group of anomalies with similar attributes is considered as a significant anomaly.

Thanks to the fact that nowadays the Bouguer anomaly can be processed in a spectral domain, it is possible to use more effective wavelength (wavenumber) filters, such as the low/high-pass cut-off filter, continuous filter, etc. In this paper, we focused on the results of four techniques: one isolation filter and three enhancement methods. The isolation filters selected in this paper are the continuation filter and band-pass filter, and the enhancement filters are a vertical and horizontal derivative and an analytic signal.

The continuation filter—upward or downward—is used to project the gravity anomaly on different surfaces, above or below the originally observed level [31,32]. We used an upward filter, which is one of the low-wavenumber pass filters, and this allowed us to calculate the Bouguer anomaly from the original observation level to the higher surface (Equation (2)).

$$L(k) = e^{-2\pi hk} \quad (2)$$

k —wavenumber [cycle/ground unit],

h —distance to upward continue [ground unit].

It is shown that the filter reduces the weight of anomalies from shallow sources in favor of deeper and larger sources. This is why, together with the increase of distance h , visibility of the shallow anomalies decreases. It can be said that this is one of the isolated filters that extracted a regional anomaly, connected with deeper geological sources from the Bouguer anomaly.

As the result of the upward continuation filter, a regional anomaly is often used to calculate residual anomalies connected with shallow geological sources. This regional

anomaly is subtracted from the Bouguer anomaly to calculate the residual anomalies. Because this filter is found to be a clear filter, it is more probable that residual anomalies should not be overinterpreted near the edge of the research area.

The next filters use derivatives and analytic signal methods. All of them are used to detect and bring out linear structures and structure edges, very often almost invisible in the Bouguer or residual anomalies distribution. They are known to emphasize the perceptibility of the anomalies based on the higher wavenumber component of those anomalies, which means that they are produced by geological contacts and boundaries.

Vertical derivatives are especially foreordained to bring out the shallow anomaly, while horizontal derivatives are used to delineate the structure edges and lineaments [33,34]. In this paper, the first vertical VDR and total horizontal THDR derivatives are used and mathematically calculated from the Bouguer anomaly using formulas VDR (3), THDR (4).

$$\text{VDR} = (\partial g / \partial z)^{1/2} \quad (3)$$

where g is the Bouguer anomaly,

And

$$\text{THDR} = [(\partial g / \partial x)^2 + (\partial g / \partial y)^2]^{1/2} \quad (4)$$

Another type of derivative technique is the total derivative, known as the 3D analytic signal amplitude, and the first order of ASA is calculated as (5) [35]:

$$\text{ASA} = [(\partial g / \partial x)^2 + (\partial g / \partial y)^2 + (\partial g / \partial z)^2]^{1/2} \quad (5)$$

4. Results

The research was based on gravity data from a data base of the Polish Geological Institute–National Research Institute.

4.1. Bouguer Anomalies

In gravimetric studies, Bouguer anomalies are the basis for the interpretation of the geological structure of the rock. For their correct calculation, it is necessary to introduce the Bouguer reduction into the measured values of gravity. According to Formula (1), the reduction consists of several individual corrections. One of them is the Bouguer correction, whose value depends on the average bulk density of the formations that form the near-surface part of the rock sequence. In calculations for areas with a large horizontal extent, the average density of the earth's crust is usually used, which is $2.67 \text{ g}\cdot\text{cm}^{-3}$. However, taking into account the fact that the entire study area is made of Carpathian flysch, its average bulk density was used for the calculations [36]. Analyzing the range of density variability in individual units of the Western Flysch Carpathians [37] and data from boreholes [38], the average density of the Carpathian flysch was assumed to be $2.5 \text{ g}\cdot\text{cm}^{-3}$ for the calculations of the Bouguer correction. Due to the mountainous nature of the study area, it was necessary to take into account the second correction, the terrain correction, in the calculations of the Bouguer anomaly. Since this correction also requires an a priori value of the mean density of near-surface rocks, its value was the same as in the case of the Bouguer correction, i.e., $2.5 \text{ g}\cdot\text{cm}^{-3}$. Terrain correction was calculated within a radius of 20 km around the gravimetric measurement point based on the DEM (Digital Elevation Model), with a resolution of $25 \text{ m} \times 25 \text{ m}$, downloaded from the Copernicus portal, which is part of the European Union's Space Programme. Taking into account all necessary corrections, it was possible to calculate the value of the Bouguer anomaly (Figure 3).

The change in the value of the Bouguer anomaly is visible in the general direction from north to south. Going from the north of the analyzed area, the value of the anomaly decreases towards the south, and then begins to increase, which should be associated with the deep bedrock. The lowering of the anomaly value from north to south reflects the collapse of the crystalline European Plate in this direction, i.e., the increase in thickness of the lighter flysch formations. In turn, the renewed increase in value correlates well

with the emergence of the crystalline ALCAPA Plate, and thus with the reduction in the thickness of the lighter Podhale flysch formations. The range of variability of the Bouguer anomaly value is significant and ranges from -61 mgal to -12 mgal, which largely masks smaller anomalies in amplitude originating from smaller geological structures. Thus, only anomalies with significant horizontal extents and greater amplitudes are visible in the distribution of anomalies.

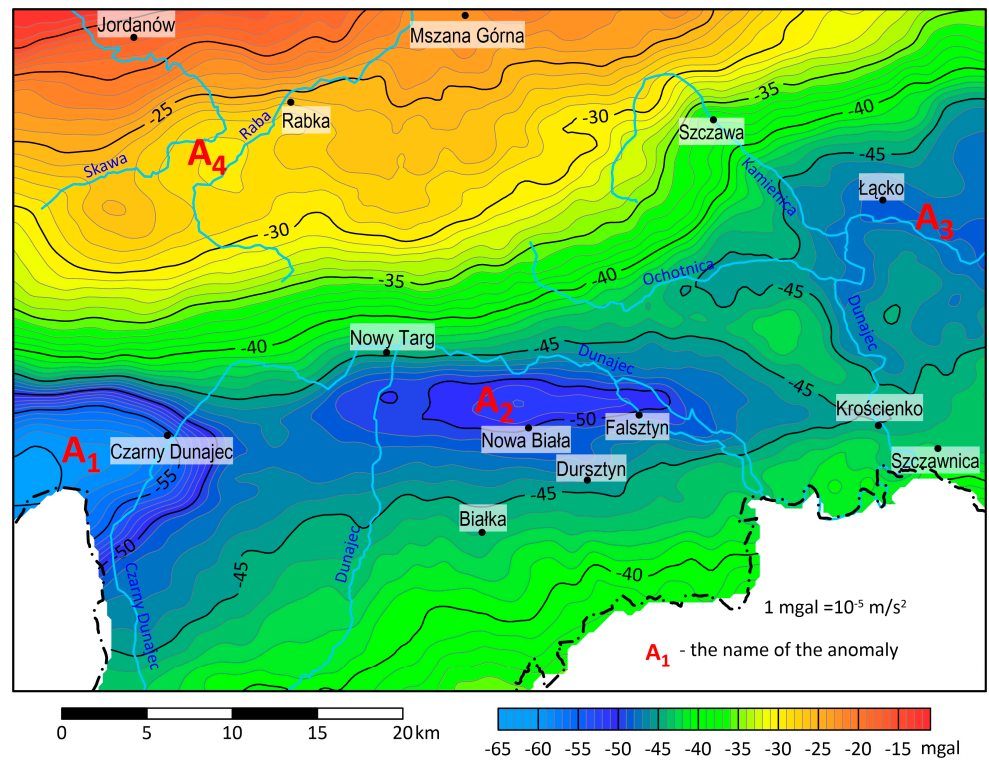


Figure 3. Distribution of Bouguer anomalies.

At the negative extreme of the Bouguer anomaly, three latitudinal extent anomalies A_1 , A_2 , and A_3 are visible. The first two clearly correlate with the Orava-Nowy Targ Basin; the western A_1 anomaly is generated by the Orava Basin, while the eastern A_2 is generated by the Nowy Targ Basin. The formations of both basins are less dense than the surrounding rocks, resulting in relatively negative anomalies. To the west of the interpreted area, there is an extensive, relatively negative, A_3 anomaly with much smaller amplitude anomalies of two basins mentioned above. In the northern part of the research area, south of the town of Rabka, a relatively negative anomaly A_4 is visible. Its small surface range and amplitude smaller than the basin anomalies means that its source is a structure of a size and depth smaller than the Orava-Nowy Targ Basin. The anomalies A_3 and A_4 perhaps indicate a thicker pile of the Outer Carpathian flysch above the basement of the North European Plate. They are probably linked to deep faults reaching the basement. Some Neogene deposits are also possible below the Carpathian's thrusts.

4.2. Residual Anomalies

The shape of the Bouguer anomaly, which is significantly influenced by the deep basement, makes the influence of local geological and tectonic structures hardly visible or invisible on the anomaly distribution (Figure 3). For this reason, isolation techniques are used to isolate the regional (large scale) and residual (local scale) anomalies connected accordingly with the deep and shallow sources. To divide the regional anomaly, an upward continuation filter was used to calculate the Bouguer anomaly of the surface 3000 m above the original level (Figure 4). The obtained regional anomaly distribution confirms the previously described relationship between the Bouguer anomaly and the general geological

structure and reflects the shape of the crystalline basement. Subtraction of the regional field from the Bouguer anomaly allowed us to obtain the distribution of residual anomalies as the closest mathematical approximation to real local anomalies (Figure 5).

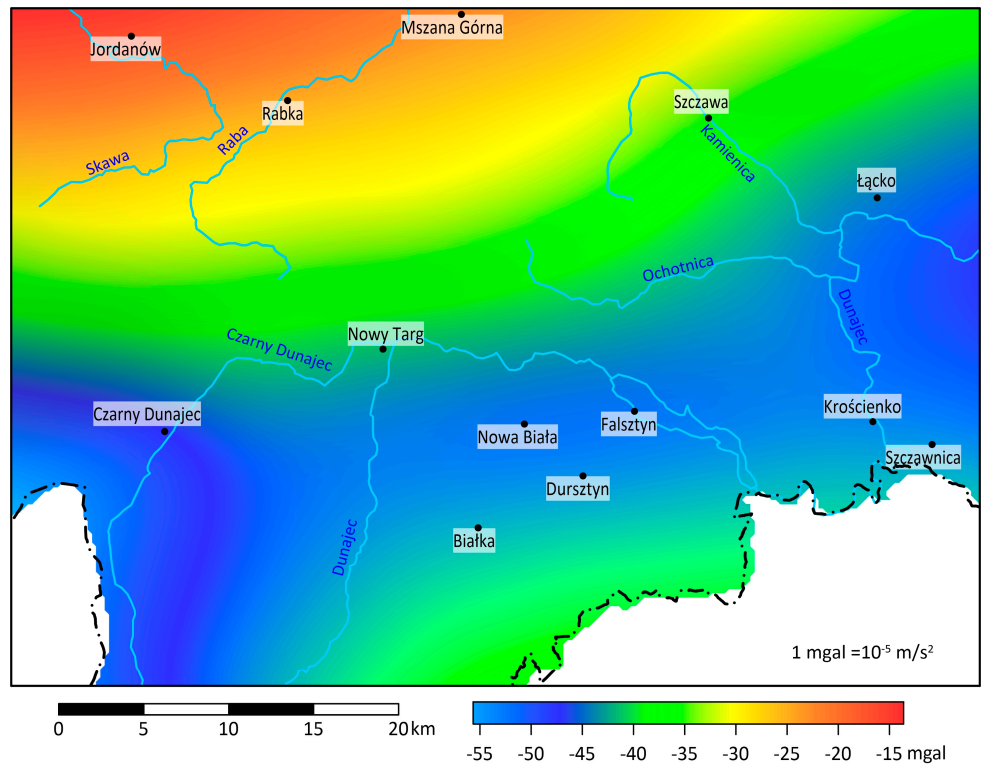


Figure 4. Distribution of regional anomalies.

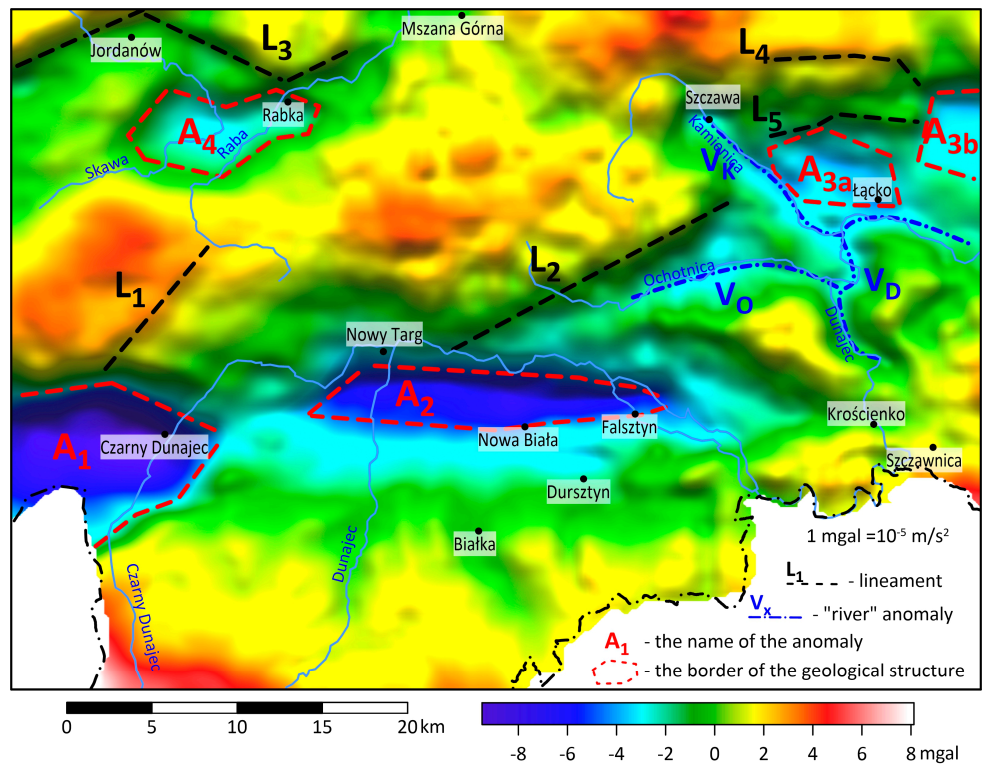


Figure 5. Distribution of residual anomalies.

The removal of the regional field emphasized anomalies A_1 and A_2 within the Orava-Nowy Targ Basin, which bring two standalone basins out: the Orava Basin and the Nowy Targ Basin, separated by the Ludźmierz Elevation. The horizontal range and amplitudes of anomalies generated by both basins clearly indicate that the Orava Basin is deeper than the Nowy Targ Basin. This conclusion is confirmed by drillings [39] and seismic surveys [8]. Based on the distribution of anomalies generated by both basins, it is possible to determine the approximate location of the faults that limit the basin (Figure 5, red dashed lines). It is characteristic that, for both basins, the values of anomalies decrease faster at their northern border than at the southern one. This may indicate that in the northern part, the shore of the basin is steeper, that is, the bottom of the basin was thrown faster by a fault or a series of faults.

In the discussed area, narrow, linear residual anomalies are clearly visible, which correlate with the course of the rivers (Figure 4, blue dashed line).

The V_D anomaly is associated with the Dunajec River, the V_K anomaly with the Kamienica River, and the V_O anomaly with the Ochotnica River. These anomalies are probably related to the existence of alluvial deposits, the density of which is much lower than that of the surrounding flysch. It cannot be ruled out that, despite the exact NMT, the calculated terrain correction did not fully remove the influence of the complex relief. It is worth noting that, apart from these rivers, in the remaining study area, there is no correlation between anomalies and the course of the rivers.

Separation of the fields allowed us to obtain a more accurate picture of anomaly A_3 , which was previously seen on the distribution of Bouguer anomalies (Figure 3). This anomaly, or rather an anomalous region with relatively negative values, has a much more complicated shape than anomalies A_1 and A_2 . Above the village of Łącko, a negative anomaly A_{3a} is visible, which cannot be correlated with the Dunajec River. Furthermore, there was a negative anomaly A_{3b} , which has clear boundaries that may correspond to faults.

In terms of the distribution of residual anomalies, the Pieniny Klippen Belt is very poorly visible, and only its northern border, which is the border with the Nowy Targ Basin, is clearly marked. It is worth noting that to the east of Dursztyn, lower values of the residual anomaly are observed than to the west. These values may indicate that the average bulk density of rocks in this region is lower than in the rest of the PKB area. This very well corresponds with the type of rocks in the PKB research area—in the western part, a mixture of different sedimentary rocks and in the eastern part, limestones. The southern boundary of the Pieniny Klippen Belt with the Podhale flysch is either invisible or very poorly visible, probably due to the small density contrast between the two geological structures [2,22].

In addition to the anomalies described above, several lineaments and density borders can be distinguished in the study area. Two lineaments, L_1 and L_2 , can be observed in the Krynica Unit of the Magura Nappe (Figure 5, black dashed line), which have a similar SW-NE azimuth, with L_1 originating at the northern border of the Orava Basin and L_2 at the northern border of the Nowy Targ Basin. It seems that these lineaments are a reflection of deeper faults that constitute density boundaries. North of Jordanów, at its northern border, the L_3 density boundary is visible, which runs partly in the Rača Unit and partly on its border with the Bystrica Unit. Above the highlighted anomaly A_{3a} , east of the village of Szczawa, two lineaments L_4 and L_5 can be distinguished, which coincide with the boundaries of overthrusts within the Bystrica Unit.

The Naprawa-Skawa Dolna fault and its extension, the Rokiciny-Lasek fault with a strike almost perpendicular to the overthrusts, are not marked at all in the anomaly distribution. The second fault of a similar course, the Dunajec fault, is visible only in fragments. In general, it can be stated that the NNW-SEZ faults are practically invisible. The distribution of residual anomalies also does not allow us to separate the boundaries of the Mszana Górna window. Thus, the formations in the window area do not differ in terms of density from those of the adjacent areas.

4.3. Gravity Vertical Derivative (VDR)

To bring out the significant anomaly and accent their perceptibility, enhancement techniques are used, in particular the vertical and horizontal derivative and the analytic signal. In the first step, the gravity vertical derivative was calculated (Figure 6), which generally allows us to emphasize the shallow changes in density.

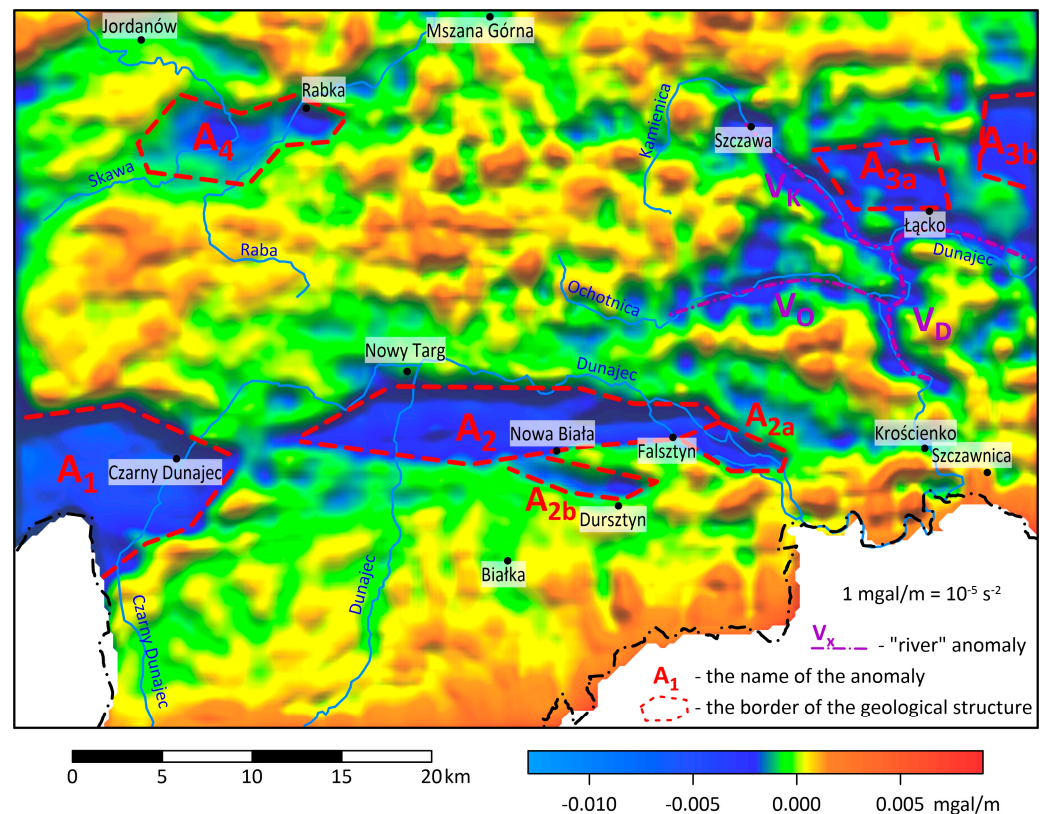


Figure 6. Distribution of gravity vertical derivative (VDR). (The color scale corresponded to the best visibility of the zones).

Both basins—the Orava (A_1) and the Nowy Targ (A_2)—are clearly visible in the distribution of anomalies. The meridional sections of both anomalies confirm that the northern edges of the basins dip steeper than the southern ones. The designated anomaly boundaries, especially the northern one, provide a better location of the actual tectonic boundaries of the basins. It should be noted that the southern border of the A_2 anomaly does not coincide with the location of the border between the PKB and the Nowy Targ Basin. The deposits in the basin cover the northern boundary fault (blind fault) of the PKB [2].

To the south and east of the A_2 anomaly, two smaller anomalies A_{2a} and A_{2b} appeared as the continuation of the Nowy Targ Basin. Both anomalies indicate shallow deposits with a lower density than their surroundings. These anomalies are located in the valleys of the Białka and Dunajec rivers and are filled with significant amounts of Quaternary pebbles. These pebbles are mined at the Frydman Plant. The artificial Czorsztyn lake is located in anomaly A_{2a} , while anomaly A_{2b} indicates the location of the ancient valley of the Białka River.

The decomposition of the vertical gravity derivative confirms the existence of the previously discussed anomalies A_{3a} and A_{3b} . On the other hand, Rabka Basin A_4 is less visible, indicating the small thickness of the formations that fill it. The previously isolated anomalies of V_D , V_K , and V_O are clearly visible. The distribution of the vertical derivative confirms that they are undoubtedly associated with river valleys and most likely that they originate from light alluvial formations.

4.4. Total Horizontal Derivative (THDR) and Analytic Signal (ASA)

To separate the boundaries of geological or tectonic structures (lineaments), a horizontal derivative (THDR) and an analytical signal (ASA) were used. In both methods, the lineaments are determined on the basis of their local maxima. It can be seen on the THDR distribution (Figure 7) that more lineaments were determined than based on the distribution of residual anomalies (Figure 5).

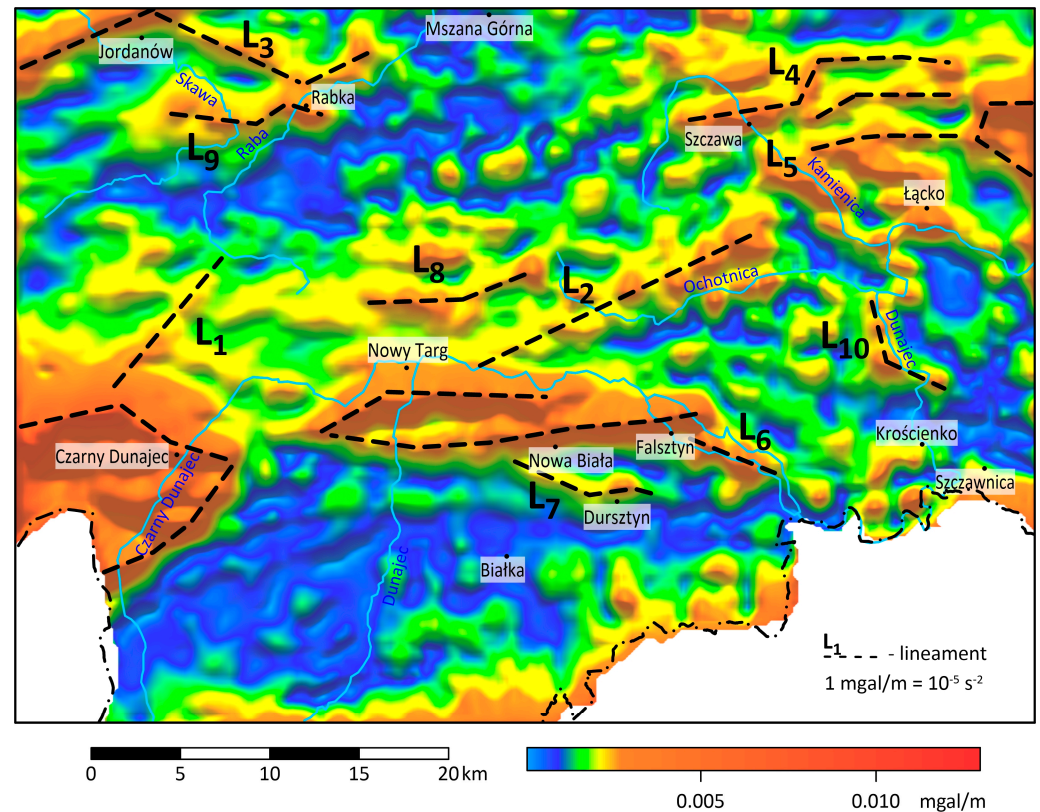


Figure 7. Distribution of gravity total horizontal derivatives (THDR).

Lineaments contouring the boundaries of the Orava Basin and the Nowy Targ Basin are well visible. To the south of the latter, lineaments L_6 and L_7 were identified. Lineament L_6 marks the southern boundary of the structure, with reduced density A_{2a} recorded in the distribution of the vertical derivative, and lineament L_7 marks the southern boundary of the structure A_{2b} (Figure 6).

North of both basins, the existence of lineaments L_1 and L_2 is confirmed. Lineament L_8 with a latitudinal course is drawn between them. It has no correlation with relief and known geological boundaries. In the early recorded anomalies A_{3a} and A_{3b} (Figures 5 and 6), only the northern boundaries of the structures generating these anomalies are visible. The L_4 and L_5 lineaments interpreted earlier are also clearly visible, but their course has become much more complicated, which proves the nature of the geological and tectonic structure of this area.

In the THDR image from the boundaries of the A_4 anomaly in the Rabka Valley area, only the northern boundary of the structure (lineament L_9) is well reproduced. To the north of it, the existence of an earlier L_3 lineament is confirmed. A small L_{10} lineament can also be distinguished along the Dunajec Fault.

The transfer of the lineaments extracted in the THDR procedure to the distribution of the analytical signal (Figure 8) shows that they coincide with the structures visible on the ASA distribution, although some of them are marked slightly weaker, such as the L_8 lineament or the L_4 – L_5 group. This can be related to the fact that ASA as a total derivative is calculated taking into account the vertical derivative, which emphasizes shallower, even small structures, making the distribution of ASA more disturbed.

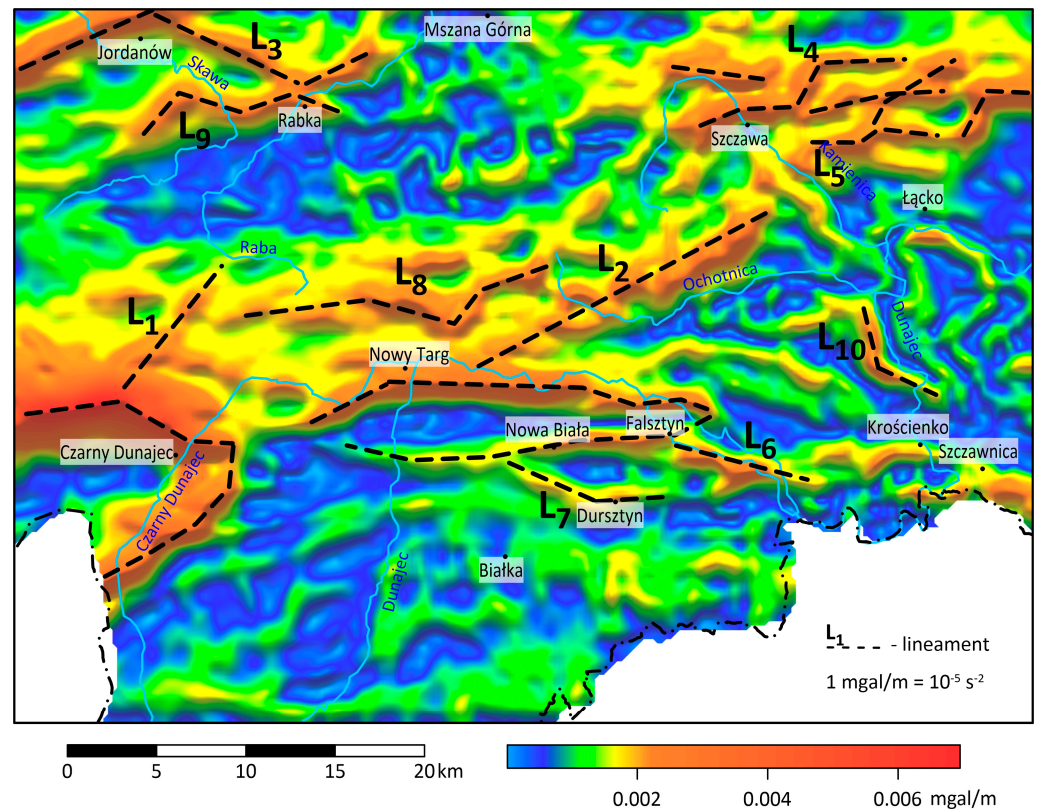


Figure 8. Distribution of gravity analytic signals (ASA).

5. Discussion and Conclusions

The interpretation of gravimetric studies was carried out for the area, which covered both the Outer and Inner Carpathians. As presented above, both geological formations are separated by the Pieniny Klippen Belt, and therefore the research area had a complicated geological structure. Since gravimetric studies reflect the spatial distribution of bulk density, gravimetric interpretation was particularly difficult because of the regular stratification of the Outer (Flysch) Carpathians.

Almost the entire research area was located in a mountainous area; despite the introduction of terrain correction, some boundaries and lineaments (especially those that run through the top parts of the mountains) could have been incorrect. To verify the results, all the interpreted boundaries of the structures and lineaments were applied to the terrain digital model of the research area (Figure 9). The analysis did not show a significant effect of morphology on the results obtained.

The general distribution of Bouguer anomalies reflects the basement and is consistent with the general geological setting. The distribution confirms the dip of the crystalline European plate and the surface of the ALCAPA plate, whereas the Pieniny Klippen Belt is less distinguished. The southern contact of the PKB with the ALCAPA plate is practically invisible, which indicates a very similar bulk density of both geological structures at the study site. The northern border of the PKB correlates well with the contact of the Nowy Targ Basin, which, like the Orava Basin, is clearly visible in the distribution of gravity anomalies.

The general geological structure is also well seen in the distribution of regional anomalies, which were calculated and then removed from Bouguer's anomalies to emphasize smaller local structures. The obtained distribution of the residual anomaly not only better demonstrated both of the basins mentioned above (anomalies A₁ and A₂) but also allowed us to determine the unknown boundaries of lighter formations in the Rabka Basin and an area located north of the village Łącko (the anomaly A₄). It is worth noting that the boundaries of the basins do not fully coincide with the morphology of the terrain (Figure 9).

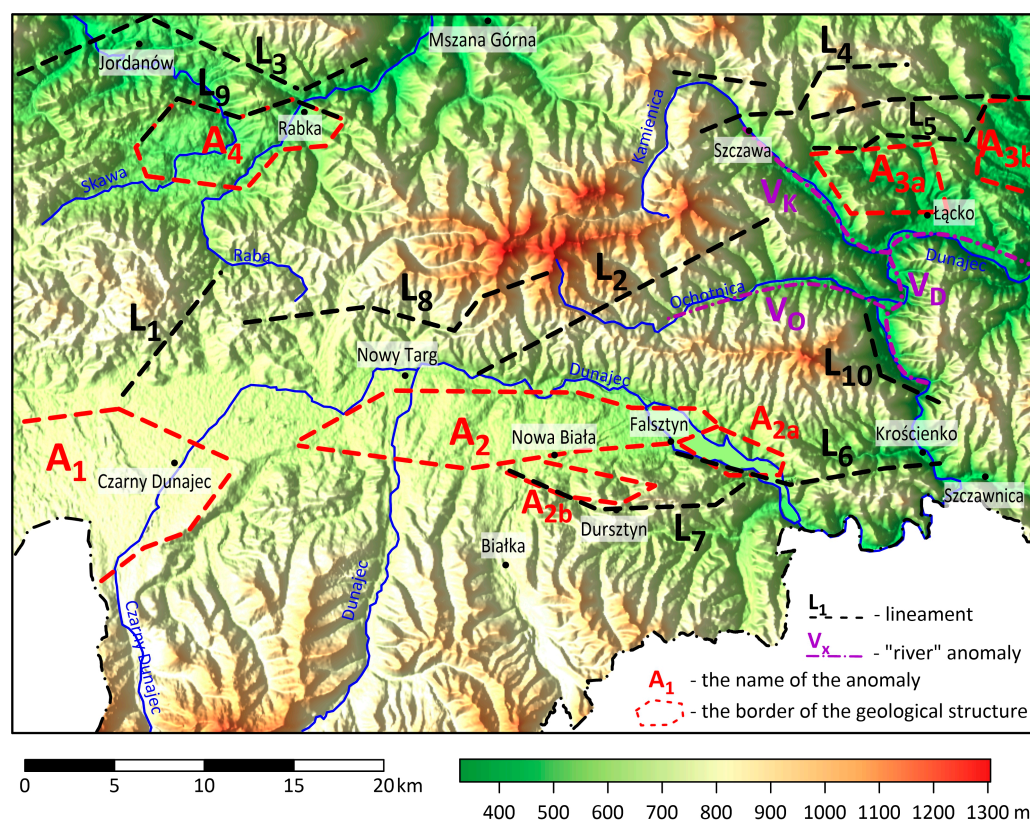


Figure 9. Distribution of the digital terrain model (DTM) with interpreted lineaments.

The confirmation of the above structures and refinement of their boundaries was obtained by analyzing the distribution of the vertical gravity derivative. This distribution also allowed us to determine the boundaries of new formations A_{2a} , A_{3a} , and A_{3b} . The area of anomaly A_{2a} contains lighter deposits located in the ancient valley of the Białka River. The unknown formations A_{3a} and A_{3b} also contain lighter deposits than surrounding rocks.

Based on the distribution of the residual anomaly, several lineaments were determined reflecting the density limits. In addition, the total horizontal derivative and analytic signal distributions were calculated and plotted, which makes it easier to identify the discovery of the boundaries of geological structures and the course of faults. Both methods confirmed and refined the course of the designated lineaments, as well as the existence of others.

The faults shown in Figure 2 are completely invisible, except for a fragment of the Dunajec fault (the lineament L_{10}). A group of lineaments L_4 and L_5 are generally known, but other lineaments were discovered during this research. Some of these lineaments may be the result of deeper subsurface faults, particularly L_1 and L_2 . A confirmation of all lineaments is possible by seismic research.

Author Contributions: Conceptualization, S.P., M.L. and J.G.; methodology, M.L.; software S.P. and M.L.; validation, S.P., M.L. and J.G.; formal analysis, S.P., M.L. and J.G.; resources, S.P. and J.G.; data curation, S.P. and M.L.; writing—original draft preparation, S.P. and J.G.; writing—review and editing, S.P. and M.L.; visualization, S.P. and M.L.; supervision, J.G. All authors have read and agreed to the published version of the manuscript.

Funding: This research was funded by NATIONALE SCIENCE CENTRE Poland, grant number 2019/35/B/ST10/00241.

Data Availability Statement: Not applicable.

Conflicts of Interest: The authors declare no conflict of interest.

References

1. Golonka, J.; Pietsch, K.; Marzec, P. The North European Platform suture zone in Poland. *Geol. Geophys. Environ.* **2018**, *44*, 5–16. [[CrossRef](#)]
2. Golonka, J.; Pietsch, K.; Marzec, P.; Kasperska, M.; Dec, J.; Cichostępski, K.; Lasocki, S. Deep structure of the Pieniny Klippen Belt in Poland. *Swiss J. Geosci.* **2019**, *112*, 475–506. [[CrossRef](#)]
3. Golonka, J.; Gawęda, A.; Waškowska, A. Carpathians. In *Encyclopedia of Geology*, 2nd ed.; Alderson, D., Elias, S.A., Eds.; Elsevier: Amsterdam, The Netherlands, 2021; pp. 372–381. [[CrossRef](#)]
4. Golonka, J.; Waškowska, A.; Ślącza, A. The Western Outer Carpathians: Origin and evolution. *ZDGG—Z. Dtsch. Ges. Geowiss.* **2019**, *170*, 229–254. [[CrossRef](#)]
5. Urbaniec, A.; Bajewski, Ł.; Bartoń, R.; Wilk, A. Analysis of the seismic image for the Carpathians and their basement resulting from the reprocessing of 2D seismic profiles. *Nafta-Gaz* **2018**, *74*, 563–574. [[CrossRef](#)]
6. Stefaniuk, M.; Klityński, W.; Jarzyna, J.; Golonka, J. The structure of the Carpathian overthrust and its basement in the Polish Western Carpathians in the light of reinterpretation of selected regional magnetotelluric profiles. *Geologia* **2007**, *33*, 143–166.
7. Grabowska, T.; Bojdys, G.; Lemberger, M.; Medoń, Z. Geophysical-and-geological interpretation of gravity and magnetic anomalies in Polish Western Carpathians. *Geologia* **2007**, *33*, 103–126.
8. Pomianowski, P. Tektonika Kotliny Orawsko-Nowotarskiej—wyniki kompleksowej analizy danych grawimetrycznych i geoelektrycznych. *Prz. Geol.* **2003**, *51*, 498–506, (In Polish, English Summary).
9. Barmuta, J.; Mikołajczak, M.; Starzec, K. Constraining depth and architecture of the crystalline basement based on potential field analysis—The westernmost Polish Outer Carpathians. *J. Geosci.-Czech* **2019**, *64*, 161–177. [[CrossRef](#)]
10. Mikołajczak, M.; Barmuta, J.; Ponikowska, M.; Mazur, S.; Starzec, K. Depth-to-basement study for the western Polish Outer Carpathians from three-dimensional joint inversion of gravity and magnetic data. *J. Geosci.-Czech* **2021**, *66*, 15–36. [[CrossRef](#)]
11. Telford, W.M.; Geldart, L.P.; Sheriff, R.E. *Applied Geophysics*, 2nd ed.; Cambridge University Press: Cambridge, UK, 1990; p. 770. [[CrossRef](#)]
12. Mallick, K.; Vasanthi, A.; Sharma, K.K. Gravity Method in Structural Studies. In *Bouguer Gravity Regional and Residual Separation: Application to Geology and Environment*; Springer: Dordrecht, Germany, 2012. [[CrossRef](#)]
13. Guglielmetti, L.; Moscariello, A. On the use of gravity data in delineating geologic features of interest for geothermal exploration in the Geneva Basin (Switzerland): Prospects and limitations. *Swiss J. Geosci.* **2021**, *114*, 15. [[CrossRef](#)]
14. Cooper, G.R.J. The extraction of edges and ridges from potential field data using gradient vector information. In *Proceedings of the Numerical Analysis and Applied Mathematics ICNAAM 2012: International Conference of Numerical Analysis and Applied Mathematics*, Kos, Greece, 19–25 September 2012; Volume 1479, pp. 2200–2203. [[CrossRef](#)]
15. Chen, G.; Liu, T.; Sun, J.; Cheng, Q.; Sahoo, B.; Zhang, Z.; Zhang, H. Gravity method for investigating the geological structures associated with W-Sn polymetallic deposits in the Nanling Range, China. *J. Appl. Geophys.* **2015**, *120*, 14–25. [[CrossRef](#)]
16. Golonka, J.; Gahagan, L.; Krobicki, M.; Marko, F.; Oszczytko, N.; Ślącza, A. Plate Tectonic Evolution and Paleogeography of the Circum-Carpathian Region. In *The Carpathians and Their Foreland: Geology and Hydrocarbon Resources*; Golonka, J., Picha, F., Eds.; American Association of Petroleum Geologists: Tulsa, OK, USA, 2006; Volume 84, pp. 11–46. [[CrossRef](#)]
17. Gawęda, A.; Golonka, J. Variscan plate dynamics in the circum-carpathian area. *Geodin. Acta* **2011**, *24*, 141–155.
18. Kowal-Kasprzyk, J.; Waškowska, A.; Golonka, J.; Krobicki, M.; Skupien, P.; Słomka, T. The Late Jurassic–Palaeogene Carbonate Platforms in the Outer Western Carpathian Tethys—A Regional Overview. *Minerals* **2021**, *11*, 747. [[CrossRef](#)]
19. Golonka, J.; Gawęda, A.; Waškowska, A.; Chew, D.; Szopa, K.; Drakou, F. Tracing Pre-Mesozoic Tectonic Sutures in the Crystalline Basement of the Protocarpathians: Evidence from the Exotic Blocks from Subsilesian Nappe, Outer Western Carpathians, Poland. *Minerals* **2021**, *11*, 571. [[CrossRef](#)]
20. Birkenmajer, K. Stages of structural evolution of the Pieniny Klippen Belt, Carpathians. *Stud. Geol. Polon.* **1986**, *88*, 7–32.
21. Birkenmajer, K. Exotic Andrusov Ridge: Its role in plate-tectonic evolution of the West Carpathian Fold-belt. *Stud. Geol. Polon.* **1988**, *91*, 7–37.
22. Golonka, J.; Waškowska, A.; Cichostępski, K.; Dec, J.; Pietsch, K.; Łój, M.; Bania, G.; Mościcki, W.J.; Porzucek, S. Mélange, Flysch and Cliffs in the Pieniny Klippen Belt (Poland): An Overview. *Minerals* **2022**, *12*, 1149. [[CrossRef](#)]
23. Golonka, J.; Aleksandrowski, P.; Aubrecht, M.; Chowaniec, J.; Chrustek, M.; Cieszkowski, M.; Florek, R.; Gawęda, A.; Jarosiński, M.; Kepińska, B.; et al. Orava Deep Drilling Project and the Post Paleogene tectonics of the Carpathians. *Ann. Soc. Geol. Pol.* **2005**, *75*, 211–248.
24. Gawęda, A.; Szopa, K.; Golonka, J.; Chew, D.; Waškowska, A. Central European Variscan Basement in the Outer Carpathians: A Case Study from the Magura Nappe, Outer Western Carpathians, Poland. *Minerals* **2021**, *11*, 256. [[CrossRef](#)]
25. Barmuta, J.; Starzec, K.; Schnabel, W. Seismic-Scale Evidence of Thrust-Perpendicular Normal Faulting in the Western Outer Carpathians, Poland. *Minerals* **2021**, *11*, 1252. [[CrossRef](#)]
26. Márton, E.; Tokarski, A.; Halasz, D. Late Miocene counterclockwise rotation of the Pieniny Andesites at the contact of the inner and outer Western Carpathians. *Geol. Carpath.* **2004**, *55*, 411–419.
27. Zielińska, M. Thermal maturity of the Grajcarek Unit (Pieniny Klippen Belt): Insights for the burial history of a major tectonic boundary of the Western Carpathians. *Minerals* **2021**, *11*, 1245. [[CrossRef](#)]
28. Porzucek, S.; Loj, M. Microgravity Survey to Detect Voids and Loosening Zones in the Vicinity of the Mine Shaft. *Energies* **2021**, *14*, 3021. [[CrossRef](#)]

29. Moritz, H. Geodetic Reference System 1980. *J. Geod.* **2000**, *74*, 128–133. [[CrossRef](#)]
30. Hinze, W.J. The role of gravity and magnetic methods in engineering and environmental studies. In *Geotechnical and Environmental Geophysics, 1, Review and Tutorial*; Society of Exploration Geophysicists: Houston, TX, USA, 1990; pp. 75–126. [[CrossRef](#)]
31. Jacobsen, H. A case for upward continuation as a standard separation filter for potential-field maps. *Geophysics* **1987**, *52*, 1138–1148. [[CrossRef](#)]
32. Meng, X.; Guo, L.; Chen, Z.; Li, S.; Shi, L. A method for gravity anomaly separation based on preferential continuation and its application. *Appl. Geophys.* **2009**, *6*, 217–225. [[CrossRef](#)]
33. Ferreira, F.J.F.; de Souza, J.; de Barros e Silva Bongiolo, A.; de Castro, L.G. Enhancement of the total horizontal gradient of magnetic anomalies using the tilt angle. *Geophysics* **2013**, *78*, J33–J41. [[CrossRef](#)]
34. Cooper, G.R.J.; Cowan, D.R. Enhancing linear features in image data using horizontal orthogonal gradient ratios. *Comput. Geosci.* **2007**, *33*, 981–984. [[CrossRef](#)]
35. Roest, W.R.; Verhoef, J.; Pilkington, M. Magnetic interpretation using 3-D analytic signal. *Geophysics* **1992**, *57*, 116–125. [[CrossRef](#)]
36. Bernabini, M.; Favaro, P.; Orlando, L. Density in Bouguer anomalies and its consequences. *J. Appl. Geophys.* **1994**, *32*, 187–197. [[CrossRef](#)]
37. Adamczak, T.; Pepel, A. Characterization of physical parameters of flysch and its basement in the Carpathians area. *Geologia* **2003**, *29*, 233–251.
38. Jarzyna, J. Analysis of density and porosity measurements on cores and result of density log and Estymacja calculations in the selected wells in the West Carpathians. *Geologia* **2007**, *33*, 39–58.
39. Baumgart-Kotarba, M. On origin and age of the Orava Basin, West Carpathians. *Stud. Geomorphol. Carpatho-Balc.* **1996**, *30*, 101–116.

Disclaimer/Publisher’s Note: The statements, opinions and data contained in all publications are solely those of the individual author(s) and contributor(s) and not of MDPI and/or the editor(s). MDPI and/or the editor(s) disclaim responsibility for any injury to people or property resulting from any ideas, methods, instructions or products referred to in the content.